Journal of Hydrology (2006) **329**, 377–389

available at www.sciencedirect.com

ScienceDirect

journal homepage: www.elsevier.com/locate/jhydrol

On the use of apparent hydraulic diffusivity as an indicator of connectivity

Christen Knudby *, Jesús Carrera [1]

Department of Geotechnical Engineering and Geosciences, Technical University of Catalonia, 08034 Barcelona, Spain

Received 12 November 2004; received in revised form 15 August 2005; accepted 21 February 2006

KEYWORDS
Connectivity;
Heterogeneous media;
Diffusivity;
Pumping test;
Tracer test;
Contaminant transport

Summary Connectivity of high permeability paths is recognized as important but has not been properly quantified in the groundwater literature. In fact, it has been shown that the concept is process dependent and difficult to define so that it applies both to water flow and solute transport phenomena. Field and numerical evidence from hydraulic tests suggest that the apparent hydraulic diffusivity, D_a, could potentially inform about the phenomena. In order to test this conjecture, we present a Monte Carlo analysis based on series of fields that display varying degrees of connectivity. Our results confirm that D_a does indeed indicate the presence of connectivity. D_a is found to correlate well with early tracer arrival time, and also with the product of a flow connectivity indicator, CF, and a transport connectivity indicator, CT. This indicates that D_a accounts both for connectivity effects controlling the average plume movement (through CF) and for connectivity effects not linked to the effective medium properties that control the progression of the solute front (through CT). Analysis of seven binary fields suggests that flow connectivity hinges more on the continuity of fast paths, whereas transport connectivity seems to be more dependent on the width of connected features forming, possibly discontinuous, fast paths. In conjunction with previous studies, our results suggest that hydraulic response arrival times and early arrival times of tracer can be expected to correlate well in most types of hydrogeologic systems.

Introduction

Considerable attention has been devoted to the characterization and representation of the complex heterogeneity found in most geologic media. Connected features have received part of this attention due to their substantial impact on subsurface flow and transport. However, the concept of connectivity — how to define it, how to measure it, and under what conditions and how it affects various types of

* Corresponding author. Present address: Schlumberger-Doll Research, 320 Bent Street, Cambridge, MA 02141, USA. Tel.: +1 530 7521372; fax: +1 530 7525262.
E-mail addresses: cknudby@slb.com (C. Knudby), jesus.carrera@upc.es (J. Carrera).
[1] Tel.: +34 934016852; fax: +34 934017251.

0022-1694/$ - see front matter © 2006 Elsevier B.V. All rights reserved.
doi:10.1016/j.jhydrol.2006.02.026

hydrological response — is still being debated (e.g. Western et al., 2001; Grayson et al., 2002; Bruderer-Weng et al., 2004; Knudby and Carrera, 2005). In hydrogeology, ''connectivity'' is most often used as a reference to the physical presence of connected zones of either high or low conductivities. The closely related concepts of ''channeling'', ''preferential flow paths'', and ''early solute arrival'' are in general used as references to the effect that connectivity has on hydrological response. In this paper we use ''flow connectivity'' as a reference to a flux increase caused by connected features. Similarly, we use ''transport connectivity'' to refer to the early solute arrival as compared to the average arrival time. It is important to realize that these effects, expressed through the hydrologic response of a geological medium, may be observed even in the absence of continuous high permeability structures transversing the domain. Continuous structures are in general sufficient, but not strictly necessary for concentrated flow and early solute arrival (e.g. Sánchez-Vila et al., 1996; Fogg et al., 2000; Lee, 2004).

In a recent paper (Knudby and Carrera, 2005), we presented and analyzed indicators of statistical, flow and transport connectivity. No significant correlation was found between the three types of indicators. In other words, the assumption that a statistical measure captures the relevant aspects of connectivity should be verified before it is employed. Our results furthermore suggested that the presence of connected features can influence flow and transport differently. This points at the usefulness of treating connectivity as a process-dependent concept. Scheibe and Yabusaki (1998) present results which illustrate the potential benefits of such an approach. In short, it seems relevant to investigate the character of the relationship between flow and transport connectivity, and more specifically what role connected features play in this context.

The magnitude and spatial distribution of properties which control groundwater flow and transport are commonly estimated using pumping and tracer tests (e.g. Walton, 1987; Fetter, 2000; Meier et al., 2001; Ptak et al., 2004). Classical analytical interpretation of pumping and tracer tests is usually based on simplifying assumptions such as homogeneity, perfect layering, statistical stationarity, etc. Such assumptions facilitate interpretation, but may lead to biased parameter estimates (e.g. Gómez-Hernández et al., 1995; Meier et al., 1999; Beckie and Harvey, 2002; Sánchez-Vila and Carrera, 2004). More importantly, they do not allow extraction of all the information contained in the test results. However, if interpreted jointly or with specific attention to connectivity (e.g. Alabert et al., 1992; Herweijer, 1996a,b; Gómez-Hernández et al., 1997; Meier et al., 1998; Butler et al., 1999; Guimerá and Carrera, 2000; Fernandez-Garcia et al., 2002; Martinez-Landa and Carrera, 2005; Illman and Tartakovsky, 2005), pumping and tracer tests can improve the precision of estimates of effective flow and transport parameters and at the same time provide valuable information on heterogeneity (Vandenbohede and Lebbe, 2003). Hydraulic tomography, which consists of the joint inversion of multiple hydraulic tests while assuming the permeability to be a random function, illustrates the role of connectivity on effective parameters (Vasco et al., 2000; Yeh and Liu, 2000; Meier et al., 2001; Vesselinov et al., 2001; Bohling et al., 2002; Brauchler et al., 2003).

Sánchez-Vila et al. (1996) showed that for two-dimensional univariate log-Gaussian fields for which the high-transmissivity (T) zones are better connected than the low-T zones, the large scale effective transmissivity, T_{eff}, is consistently larger than the geometric average of the point values, T_G, which is the expected value for two-dimensional isotropic multilog-Gaussian fields (Matheron, 1967). Meier et al. (1999), Sánchez-Vila et al. (1999) illustrated that even in the presence of connected features, estimates of T_{eff} based on interpretation of pumping tests of long duration in heterogeneous media using Jacob's method (Cooper and Jacob, 1946) compare well with estimates of T_{eff} based on an assumption of mean uniform flow. In other words it is possible to get good estimates of T_{eff} from pumping tests even in the presence of significant connectivity. In this aspect, T_{eff} stands in contrast to the other parameter commonly estimated from pumping tests, the storativity, S. Schad and Teutsch (1994) used three-phased transient pumping test response to estimate the length of high-permeable lenses. They found that estimates of S obtained from Theis type curve fitting were lower for observation wells located in high-T zones than for observation wells in low-T zones. Subsequently, Herweijer and Young (1991), Herweijer (1996a,b), Meier et al. (1998) found that estimates of S obtained from Jacob's method contain information not only on near-well materials, but also on the degree of hydraulic interconnectedness between the pumping and the observation well.

All of the above studies employ an undefined and visual notion of connectivity (e.g. Grayson et al., 2002). Despite the lack of quantification, there is nevertheless substantial evidence that the storativity, S, and therefore also the hydraulic diffusivity, D ($D = T/S$), as interpreted from Jacob's method are related to connectivity, and that the relationship has to do with the presence of connected features.

In short, Jacob's method consists of plotting drawdown vs. time on a semi-logarithmic paper. Estimates of T_{eff} and subsequently S are then found by drawing a straight line through late-time points and computing

$$T_{\text{eff}} = \frac{2.3Q}{4\pi m} \tag{1}$$

$$S = \frac{2.25 T_{\text{eff}} t_0}{r^2} \tag{2}$$

where Q is the constant pumping rate, m is the slope of the straight line, t_0 is the time axis intercept, and r is the radial distance to the observation well (see e.g. Freeze and Cherry, 1979, for further details). When the observation and the pumping wells are connected by high-T features, the drawdown signal will be observed early, i.e. t_0 will be small. In other words, high connectivity is expressed through an artificially small estimate of S and consequently a large estimate of D. Heterogeneity causes estimates of storativity obtained from Jacob's method to be different from their actual values. The corresponding values of diffusivity are also affected by heterogeneity in a similar way, although they may be considered more representative of overall system

behavior. We therefore refer to the values obtained from Jacob's method as *apparent storativity*, S_a, and *apparent diffusivity*, D_a ($D_a = T_{eff}/S_a$). The effect that flow connectivity has on S_a is analogous to the effect that transport connectivity has on apparent porosity estimates from tracer tests (Guimerá and Carrera, 2000; Fernandez-Garcia et al., 2002).

Solute transport related support of the conjecture that S_a and D_a contain information on connectivity can be found in studies of Herweijer and Young (1991), Herweijer (1996a,b), Paris (2002). Herweijer (1996a) analyzed pumping test data from the MADE site and numerically simulated pumping and tracer tests for the site. Linear correlation was found between the logarithm of the travel time of the drawdown signal and the logarithm of the tracer travel time. In a similar investigation for three-dimensional fracture networks, Paris (2002) found that tracer and drawdown breakthrough time show strong correlation over distances comparable to the size of the disc-shaped fractures. The strength of the correlation was found to decrease with increasing matrix diffusion.

Based on the above, it is reasonable to conjecture that apparent storativity, S_a, and therefore also the apparent hydraulic diffusivity, D_a, as interpreted from Jacob's could be useful indicators of flow and/or transport connectivity. The objective of the present paper is to use defined and therefore quantifiable measures of connectivity to test the relevance of S_a and D_a as indicators or measures of connectivity. Also, we investigate how the two parameters are related to two indicators of flow and transport connectivity analyzed by Knudby and Carrera (2005). S_a and D_a are related through T_{eff}, which as shown by Meier et al. (1998) can be estimated even in the presence of significant heterogeneity.

Procedure

In order to test to what degree D_a can be considered an indicator of connectivity, we use the type of approach employed in several recent studies focusing on connectivity (e.g. Wen and Gómez-Hernández, 1998; Western et al., 2001; Zinn and Harvey, 2003; Knudby and Carrera, 2005). In short, we generate transmissivity fields and subsequently rearrange their T-values so as to enhance the presence of connected features. We thereby obtain sets of fields for which one field is (visually) better connected than the other field. In order to facilitate the analysis of apparent vs. actual properties, we assign a constant value of actual S to our fields. Next, we compute values of D_a and of a flow connectivity indicator and a transport connectivity indicator, both analyzed in (Knudby and Carrera, 2005). Finally, we analyze how the values of the connectivity indicators change as a result of the rearrangements, and how they correlate with each other.

Thus, the numerical procedure employed in this paper consists of the following steps:

1. Generation of poorly connected and well-connected fields with identical histograms.
2. Simulation of steady state and transient flow and advective transport for all fields.
3. Computation of a flow connectivity indicator and a transport connectivity indicator for all fields.
4. Computation of the apparent diffusivity for all fields.

Each of these steps is described in the following.

Generation of fields with high and low connectivity

An analysis of a concept as complex as connectivity, is likely to benefit in clarity from the use of relatively simple fields. We therefore base our analysis on two-dimensional fields which are easily manipulated to allow for varying degrees of heterogeneity. While the step from two to the more realistic three dimensions increases connectivity (e.g. Fogg, 1986; Silliman, 1996) the concept of connectivity can be considered independent on dimension. Our approach is similar to the approach used in most recent studies on connectivity (Sánchez-Vila et al., 1996; Wen and Gómez-Hernández, 1998; Western et al., 2001; Zinn and Harvey, 2003; Neuweiler and Cirpka, 2005).

In order to obtain fields with low connectivity, we generate series of multi-Gaussian (MG) fields. MG-fields exhibit maximum entropy and low connectivity of extreme values (e.g. Journel and Deutsch, 1993; Gómez-Hernández and Wen, 1998). The MG-fields were generated using the sequential Gaussian simulation subroutine SGSIM (Deutsch and Journel, 1992). A total of eight series of 50 fields were generated. Each field had the dimensions of 128×128 grid cells. The eight series displayed isotropic Gaussian variogram ranges of 8, 16, 32, and 64 grid cells and $Y = \log(T)$ variances of 1.0 and 15.9 (i.e. $\log_{10}(T)$ variances of 1 and 3). T_G equals unity for all fields.

In order to generate fields with a connectivity higher than that of the MG-fields, we modified the T-distributions of the MG-fields without changing the histograms. Two different methods were used for the rearrangement. Fig. 1 shows an original MG-field (Fig. 1, center) and the two modified univariate-Gaussian fields obtained using the two rearrangement methods. Notice that both methods rearrange the T-values in such a way that strings of high-T cells are produced. The first rearrangement method (method C, see Fig. 1, left) places high-T values where the original MG-field has intermediate values. Since intermediate values tend to be well connected in MG-fields, this rearrangement method creates channels of high-T values. The method is presented by Zinn and Harvey (2003). The second method (method F, see Fig. 1, right) rearranges the T-values in such a way that linear ''fractures'' are created. Both methods are described in more detail by Knudby and Carrera (2005). In the following, ''MG-fields'' refers to the original multi-Gaussian fields, whereas ''C-fields'' (C for ''channels'') and ''F-fields'' (F for ''fractures'') refer to the fields obtained using rearrangement method C and F, respectively.

Simulation of steady state and transient flow and advective transport

Steady state and transient flow was simulated for all eight series each consisting of 150 fields (50 MG-fields, 50 C-fields, and 50 F-fields). The finite-difference code MODFLOW-2000

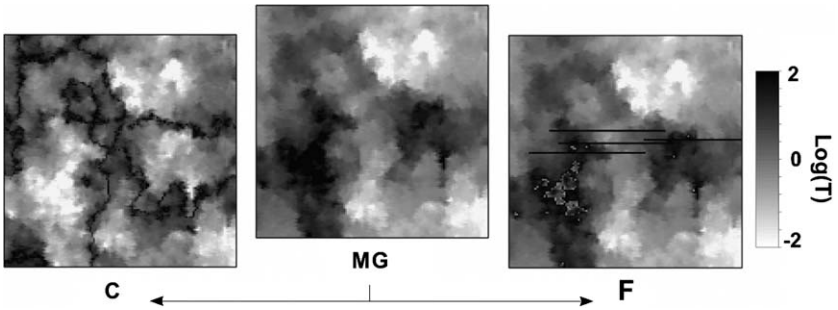

Figure 1 An original multi-Gaussian transmissivity distribution and the two corresponding distributions obtained using rearrangement methods C and F.

(Harbaugh et al., 2000) was used for the flow simulations. No-flow boundary conditions were imposed on the upper and lower boundaries. Constant heads were assigned to the left and right boundaries. For the transient flow simulations, an initial head of 1 was assigned to the entire domain. At time $t = 0$, the right boundary head was instantaneously lowered to 0. The left boundary head was maintained at 1. In other words, we solve the two-dimensional flow equation

$$\frac{\partial h}{\partial t} = \nabla(D\nabla h), \quad D = \frac{T}{S} \tag{3}$$

with initial and boundary conditions given by

$$h(t = 0, x, y) = 1, \quad h(t > 0, x = 0, y) = 1,$$
$$h(t > 0, x = L_x, y) = 0 \tag{4}$$

where h is head, t is time, D is hydraulic diffusivity, and L_x is the domain length in the x-direction, see Fig. 2. Transient flow was simulated until steady state was reached. The transient flow simulations were used to determine apparent diffusivities, whereas the steady state flow conditions were used to determine block transmissivities. The block transmissivities are assumed representative of the corresponding effective transmissivities, T_{eff}. Fig. 2 illustrates the initial condition, the boundary conditions, and the head at different times after the instantaneous head drop on the right boundary.

Breakthrough curves of flux-averaged concentration resulting from a Dirac pulse input at one of the two constant head boundaries were computed from the steady state trajectories (streamlines). The position of the streamlines was determined using a flow net approach (e.g. Fogg and Senger, 1985; Anderson and Woessner, 1992) based on the so-called dual formulation (Frind and Matanga, 1985).

The variability of storativity and porosity is commonly negligible as compared to the variability of transmissivity (e.g. Meier et al., 1998; Rutqvist et al., 1998). For all flow and transport simulations, the fields are therefore considered homogeneous with respect to both actual storativity (unity), and the product of the porosity and the aquifer thickness, θL_z (10^{-3}).

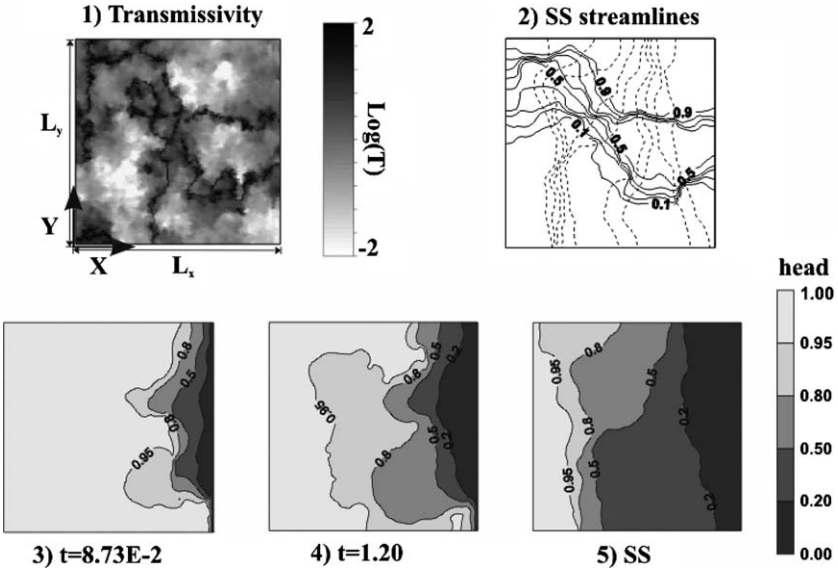

Figure 2 Transient flow simulation example. (1) Transmissivity distribution; (2) steady state (SS) streamlines and equipotential lines; (3–5) Head evolution as a result of the head drop at the right boundary. Notice the irregular head contour intervals used to emphasize the front progression.

Computation of flow and transport connectivity indicators

For all series of fields, we computed the value of a flow connectivity indicator and a transport connectivity indicator. As mentioned in the section 'Introduction', we understand by ''flow connectivity'' the degree to which flow is concentrated in high-T features. The ratio between the effective transmissivity, T_{eff}, and the geometric mean of local transmissivities, T_G, can be considered an indicator of flow connectivity (Knudby and Carrera, 2005, see also Sánchez-Vila et al., 1996; Guswa and Freyberg, 2002). We use

$$CF = \frac{T_{eff}}{T_G} \tag{5}$$

as our flow connectivity indicator. CF assumes the value 1 for two-dimensional infinite isotropic multi-Gaussian fields (Warren and Price, 1961; Matheron, 1967). We compute T_{eff} using a permeameter-type approach (also termed simple Laplacian approach by Wen and Gómez-Hernandez (1996), i.e. as the proportionality constant relating the steady state flux and the head gradient.

Transport connectivity is expressed through early solute arrival as compared to the average arrival time. As a transport connectivity indicator, we use

$$CT = \frac{t_{AVE}}{t_5} \tag{6}$$

where t_{AVE} is the average arrival time, and t_5 is the time at which 5% of the solute has arrived at the outlet. For steady state two-dimensional flow, the arrival time of the ith stream tube is $\theta L_z A_i/Q_i$, where A_i is the stream tube area and Q_i is the stream tube flow rate. t_{AVE} is the average stream tube arrival time given by

$$t_{AVE} = \theta \frac{A_{domain}}{Q_{ss}} = \theta \frac{L_x^2 L_z}{T_{eff}\Delta h} \tag{7}$$

where A_{domain} is the domain area, Q_{ss} is the steady state flow rate across the domain, θ is the porosity, Δh is the applied head difference, whereas L_z and L_x are the domain length and thickness, respectively.

In a recent study (Knudby and Carrera, 2005), we have shown that both CF and CT capture the differences in connectivity displayed by MG-, C-, and F-fields. Our results also confirmed that CF accounts for the degree to which flow is concentrated to high-T features, whereas CT accounts for early solute arrival as compared to the average arrival time. CF and CT can therefore be considered indicators of the presence of flow and transport connectivity, respectively.

Determination of apparent hydraulic diffusivity

As explained in the section 'Introduction', the interpretation of pumping tests in heterogeneous media using Jacob's method leads to estimates of S which depend on the hydraulic connection between the pumping and observation wells. We are interested in confirming and evaluating the potential utility of using D_a, as estimated using Jacob's method, as a source of information on the degree of flow and/or transport connectivity in a geologic medium. For the estimation of D_a we therefore use an approach which in a qualitative sense is similar to Jacob's method in that it assumes that S_a can be estimated from the early time hydraulic response of the system. The approach is based on a comparison of the response of a heterogeneous medium to that of a homogeneous medium. For a homogeneous medium with an actual hydraulic diffusivity, D, the flux into the domain at the left boundary produced by the sudden head drop at the right boundary, Q_{in}, is (e.g. Herrera and Yates, 1977; Carslaw and Jaeger, 1959)

$$Q_{in}(t') = Q_{ss}\left(1 + 2\sum_{n=1}^{\infty}(-1)^n e^{-n^2\pi^2 t'}\right), \tag{8}$$

$$t' = \frac{Dt}{L_x^2} \tag{9}$$

where t' is dimensionless time. For a homogeneous medium, the hydraulic diffusivity can be inferred by fitting Eqs. (8) and (9) to the observed time-dependent inflow rate. However, for a heterogeneous T-field, there will be local variations in the propagation velocity of the line of depression, especially where connected zones of high T-values are encountered, see Fig. 2.

Compared to the homogeneous case, non-uniform propagation will lead to earlier inflow increase, whereas steady state will be reached later. This is illustrated in Fig. 3. The figure displays the temporal variation of normalized inflow rates at the left boundary for three homogeneous fields assigned different values of D. The three values are $D_{eff} = T_{eff}/S$, $D_G = T_G/S$, and a calibrated value of D. T_{eff} is found from the steady state flow through the medium (using the permeameter approach described earlier), whereas T_G is the geometric mean of the point values. Also shown in the figure is $Q_{in}(t)$ obtained through numerical flow simulation. Comparison of the analytical (homogeneous) and the simulated (heterogeneous) curves shows that heterogeneity causes inflow to increase earlier, and that steady state is reached later for the heterogeneous field than for the homogeneous field with $D = T_{eff}/S$. The early arrival of the hydraulic response signal for the heterogeneous field is an expression of connectivity (similar to early arrival of solute).

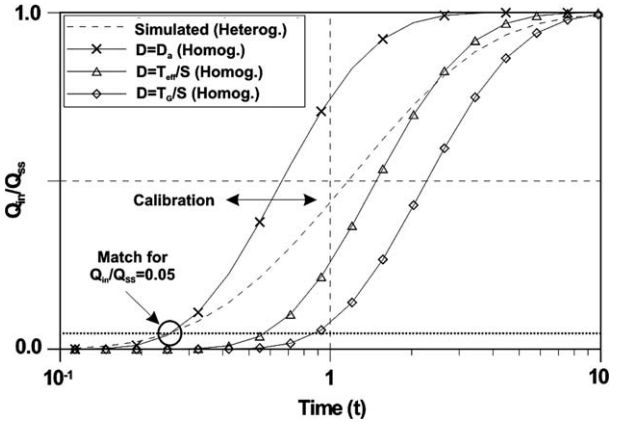

Figure 3 Temporal variation in relative inflow. The dotted line is the numerically simulated relative inflow. Full lines are analytical solutions using different diffusivities. The presented results are for the T-field depicted in Fig. 2.

In analogy with the estimation of apparent storativity using Jacob's method, we focus on the arrival of the first part of the hydraulic response signal. We therefore determine D_a as the value of D in Eq. (9) which produces a 5% relative inflow rate at the same time as the actual heterogeneous medium. The double arrow labeled ''Calibration'' indicates the iterative adjustment of the curve labeled $D = D_a$. For heterogeneous media the obtained value of D_a will always be greater than $D_{eff} = T_{eff}/S$. The time at which a match is found is in the following referred to as the ''drawdown arrival time'' or the ''hydraulic response time'', t_D, see Fig. 3. t_D corresponds to t_0 in Eq. (2). However, to clearly distinguish the drawdown arrival time, t_D, obtained from the calibration illustrated in Fig. 3 from the drawdown arrival time, t_0, obtained from a classical pumping test, we use different notation for the two parameters. For generality, we normalize D_a and in the following look at $D_R = D_a/D_G$, where $D_G = T_G/S$.

Results

To test the relevance of apparent diffusivity as a measure of connectivity, we computed the values of CF, CT, and D_R for a total of 1200 fields comprised of eight series of 50 MG-fields, 50 F-fields, and 50 C-fields. Table 1 shows that rearrangement method C is less consistent than rearrangement method F when it comes to increasing the arithmetic averages of CF, CT, and D_R. In fact, rearrangement method C causes a small, but consistent decrease in average CT for series 1—2 (for ranges equal to 8 cell sizes), and in average D_R for series 1—6 (for ranges equal to or less than 32 cell sizes). Rearrangement method C causes a consistent increase in average CF, whereas rearrangement method F consistently causes a significant increase in average CF, CT, and D_R for all series. We take this to be an indication that, although less elegant, method *F* is more consistent than method *C* in terms of creating a connectivity increase.

In order to investigate the relationship between the different measures, we analyzed the linear correlation between the logarithms of CF, CT, and D_R for the eight series of MG-, C-, and F-fields. We analyze the correlation of number pairs pertaining to either MG-, C- or F-fields. Since all fields differ only with respect to the arrangement of *T*-values, we also analyzed number pairs obtained by grouping the fields irrespective of field type. In the following, unless otherwise stated, ''correlation'' refers to the linear correlation between log-transformed values. Fig. 4 displays the values of CT vs. CF and D_R for series 3 ($\sigma_Y^2 = 1$, range=16). The first plot shows that the correlation between CF and CT is somewhat weak ($R^2 = 0.58$) when all fields are grouped. When looking at each of the three types of fields (i.e. 50 fields) separately, the correlation is even weaker ($R^2 \in [0.14;0.40]$). This indicates that unless it is used in connection with other parameters, CF cannot be expected to be particularly useful for assessing early arrival time for this series of fields. There is stronger correlation between CT and D_R ($R^2 = 0.77$) which suggests that D_R contains more information on transport connectivity than does CF for this particular series of 150 fields. In other words, D_R (preferably used in conjunction with T_{eff}) could be a valuable source of information on the tendency to early arrival. The correlation between D_R and CF (see Fig. 5) is comparable to or even stronger than between D_R and CT. This indicates that although D_R provides information on transport connectivity, it is at the same time strongly related to flow connectivity.

Table 2 lists the correlation coefficients between CT, CF, and D_R for the eight series. It is seen that qualitatively (i.e. in terms of R^2), there is little difference between the correlation found for series 3 and the remaining seven series. The correlation is consistently (for all eight series, for both 50 MG-, C-, and F-fields, and when grouping all 150 fields together) stronger between CT and D_R than between CT and CF. This supports the conjecture that D_R contains more information on the tendency to early arrival than CF, especially for well-connected fields. The effect of changes in range and variance on the correlation between the connectivity indicators is not clear. Differences in the range and variance of the MG fields affect the variance of the connectivity indicators, but leave the correlation between them largely unchanged.

The above analysis of 1200 random fields realizations document that D_R to a large degree captures connectivity

Table 1 Average values of CT, CF, and D_R for eight series of original MG-fields and rearranged C- and F-fields

Mean of CF, CT, D_R	Series #	1	2	3	4	5	6	7	8
	Range[a]	8		16		32		64	
	σ_Y^2	1.0	15.9	1.0	15.9	1.0	15.9	1.0	15.9
MG-fields	CF	0.98	1.11	1.04	1.36	1.08	1.68	0.99	1.34
MG-fields	CT	3.68	7.38	3.57	6.61	3.56	5.69	3.23	4.76
MG-fields	D_R	1.81	4.17	2.50	7.38	3.13	10.4	3.11	9.35
C-fields	CF	1.10	1.43	1.13	1.62	1.28	2.36	1.36	2.95
C-fields	CT	**2.81**	**6.09**	3.68	9.08	4.53	10.9	4.82	11.9
C-fields	D_R	**1.55**	**2.97**	**1.95**	**4.94**	**2.66**	**9.32**	3.29	14.7
F-fields	CF	2.10	6.72	2.29	10.9	2.42	12.2	2.19	10.9
F-fields	CT	8.85	18.4	8.76	15.7	8.45	15.0	7.66	13.2
F-fields	D_R	6.10	139	7.67	307	9.52	270	9.24	148

Bold font indicates a decrease when compared to the MG-fields.
[a] Range of the Gaussian variogram used to generate the 50 MG-fields.

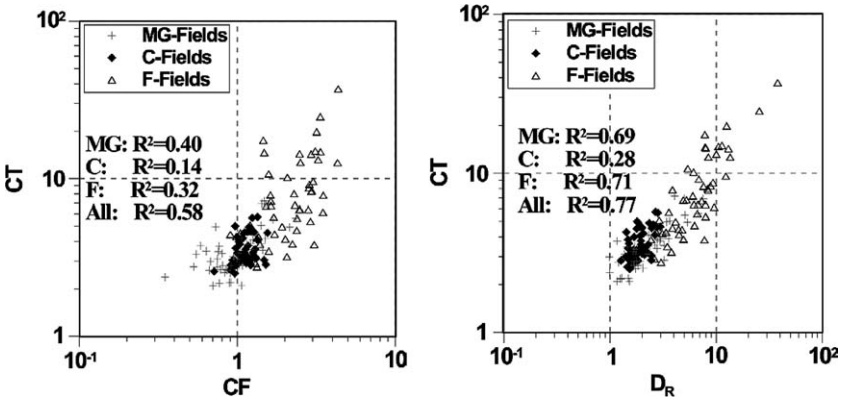

Figure 4 CT vs. CF and D_R for the 50 MG-fields, 50 C-fields, and 50 F-fields of series 3. Notice that the correlation is stronger for CT vs. D_R (R^2 = 0.77) than for CT vs. CF (R^2 = 0.58). The linear correlation coefficients are based on the log-transformed values.

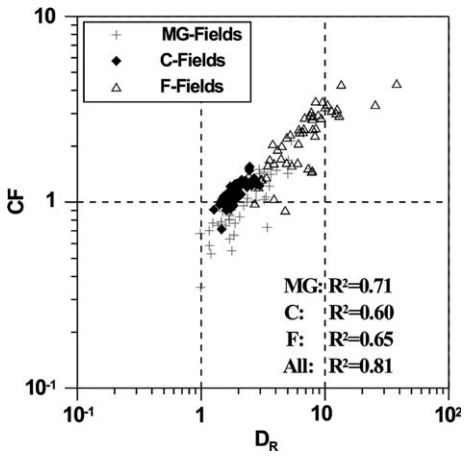

Figure 5 CF vs. D_R for the 50 MG-fields, 50 C-fields, and 50 F-fields of series 3. The linear correlation coefficients are based on the log-transformed values.

differences. This confirms previous findings that it could be useful as a means to detect and characterize connected features. The results also suggest that although D_R provides information on transport connectivity, it is at the same time strongly related to flow connectivity.

In an attempt to further analyze which factors affect D_R, CF and CT, we compared travel times of solute, t_5, and of the drawdown signal, t_D. Since D_R is computed from t_D, a comparison of t_D and t_5 could provide further information on the ability of D_R to account for early tracer arrival.

The comparison of t_D to t_5 (which is the same as $t_D \cdot T_G$ to $t_5 \cdot T_G$ for the 1200 fields as T_G = 1) in Fig. 6 illustrates that, for the eight series of 150 fields as a whole, the logarithm of the tracer arrival time is approximately linearly correlated to the logarithm of the arrival time of the drawdown signal. The slope of the trend line is 0.999. Both the strong correlation and the fact that the trend line has a slope close to 1 is in accordance with the results of Herweijer (1996b), Paris (2002).

The definition of D_R and Eq. (2) provides the following relationship between D_R and t_D (or t_0)

$$D_R = \frac{D_a}{D_G} = \frac{T_{eff}/S_a}{T_G/S} = \frac{T_{eff} \cdot S}{T_G} \frac{r^2}{2.25 \cdot T_{eff} \cdot t_D} = \frac{c_1}{T_G \cdot t_D} \tag{10}$$

where c_1 is a constant given the parameter values used in the present study. As D_R is inversely proportional to $T_G \cdot t_D$, the strong correlation between t_5 and t_D also exists between $T_G \cdot t_5$ and D_R. Furthermore, as

$$CF \cdot CT = \frac{T_{eff} \cdot t_{AVE}}{T_G \cdot t_5} = \frac{T_{eff} \cdot \theta \frac{L_x^2 L_z}{T_{eff} \Delta h}}{T_G \cdot t_5} = \frac{c_2}{T_G \cdot t_5} \tag{11}$$

where c_2 is constant given the parameter values used in the present study, the observed strong correlation between t_5 and t_D also exists between D_R and the product of CF and CT. This is illustrated in the second plot in Fig. 6.

In order to analyze in more detail the paths followed by early arriving solute and by the drawdown signal, we determined the path of least resistance (i.e., the path connecting the two permeable boundaries along which the sum of resistances, the inverse of the transmissivities, is minimum) for all fields (see Fig. 7). To this end we used a modified Dijkstra's algorithm (Dijkstra, 1959; Cherkassky et al., 1996). As one would expect, it was found that both the tracer and the drawdown signal (the fastest advancing part of the ''line of depression'') in general follows the path of least resistance. Comparison of the path of least resistance and the progression of the drawdown signal shown in Fig. 2 illustrates this.

The travel time along the path of least resistance, t_P, is approximated by the travel time along a straight path with the same resistance. That is

$$t_P = \theta \frac{L_x L_z}{T_P \frac{\Delta h}{L_P}} \tag{12}$$

where T_P is the weighted harmonic mean of the transmissivities along the path of least resistance, i.e. the effective transmissivity along that path. L_P is the length of the path. In Fig. 8 t_P is plotted against t_5 and t_D. It is seen that t_P correlates reasonably well with t_D and exceptionally well with t_5. Furthermore, t_P seems to be a good estimator of t_5 as the trend line is nearly identical to the $t_P = t_5$ line. In a previous study (Knudby and Carrera, 2005) we confirmed that the transmissivity corresponding to the percolation

Table 2 Correlation coefficients (R^2) between CT, CF, and D_R for eight series of original MG-fields and rearranged C- and F-fields and for the three types of fields together

R^2	Series #	1	2	3	4	5	6	7	8	Mean
	Range[a]	8		16		32		64		
	σ_Y^2	1.0	15.9	1.0	15.9	1.0	15.9	1.0	15.9	
MG	CF vs. CT	0.59	0.44	0.40	0.41	0.45	0.35	0.47	0.41	0.44
MG	D_R vs. CT	0.61	0.59	0.69	0.64	0.58	0.43	0.61	0.52	0.59
MG	CF vs. D_R	0.74	0.70	0.71	0.74	0.80	0.87	0.85	0.91	0.79
C	CF vs. CT	0.10	0.17	0.14	0.02	0.03	0.01	0.16	0.13	0.09
C	D_R vs. CT	0.23	0.38	0.28	0.10	0.10	0.05	0.28	0.15	0.20
C	CF vs. D_R	0.69	0.65	0.60	0.63	0.69	0.66	0.74	0.77	0.68
F	CF vs. CT	0.32	0.41	0.32	0.49	0.34	0.42	0.13	0.20	0.33
F	D_R vs. CT	0.72	0.61	0.71	0.70	0.62	0.57	0.50	0.40	0.60
F	CF vs. D_R	0.64	0.75	0.65	0.80	0.80	0.91	0.70	0.85	0.76
MG,C,F	CF vs. CT	0.65	0.58	0.58	0.55	0.49	0.44	0.39	0.37	0.50
MG,C,F	D_R vs. CT	0.85	0.79	0.77	0.66	0.63	0.50	0.59	0.46	0.66
MG,C,F	CF vs. D_R	0.86	0.81	0.81	0.81	0.82	0.86	0.79	0.85	0.82

The linear correlation coefficients are based on the log-transformed values.
[a] Range of the Gaussian variogram used to generate the 50 MG-fields.

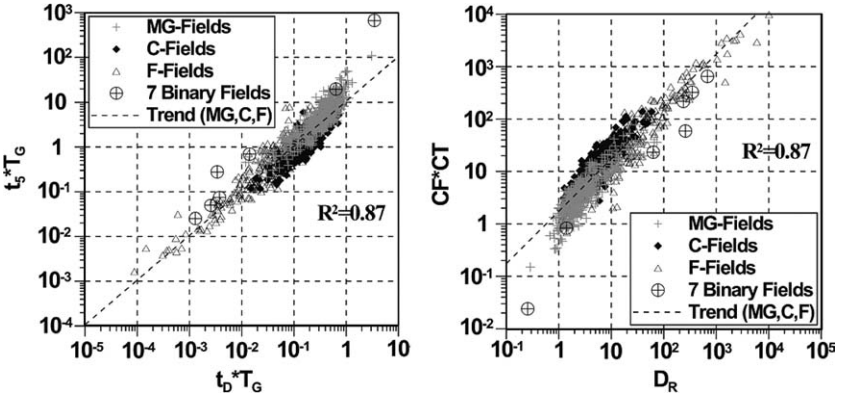

Figure 6 (1) t_5 vs. t_D for the 1200 MG-, C-, and F-fields (8 series of 150 fields) and 7 binary fields. (2) D_R vs. CF × CT for the same 1207 fields. The 7 binary fields are presented and analyzed below. The linear correlation coefficients are based on all 1200 log-transformed value pairs.

threshold of the indicator transformed field, the critical path transmissivity, T_C, (e.g. Ambegaokar et al., 1971; Hunt, 2001) was a good estimator of T_{eff}. The result that t_P appears to be a good estimator of t_5 could be considered an analogous result for advective transport. Both results suggest, in broad terms, that it can be useful to focus on the bottleneck or/and the fastest path when estimating effective properties and early arrival.

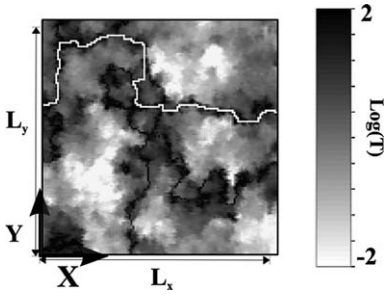

Figure 7 The path of least resistance (left↔right) for the transmissivity distribution shown in Fig. 2.

Fig. 8 shows that t_P in many cases is often significantly larger than t_5. In order to find the reason for this apparent contradiction, and at the same time analyze other aspects of the relationships between the parameters used in the present study, we analyzed the seven binary fields depicted in Fig. 9. The fields are constructed to help analyze the effect of a low-T barrier (fields F1—F3, and F4—F5), the influence of channel width (fields F1, F6, F7 — the three fields have the same T_G and T_{eff}), and what affects travel time besides the path of least resistance (F1 vs. F5 and F3 vs. F4). The results of the analysis of the binary fields, which are presented in Table 3, illustrate some fundamental differences between flow connectivity, transport connectivity and apparent diffusivity.

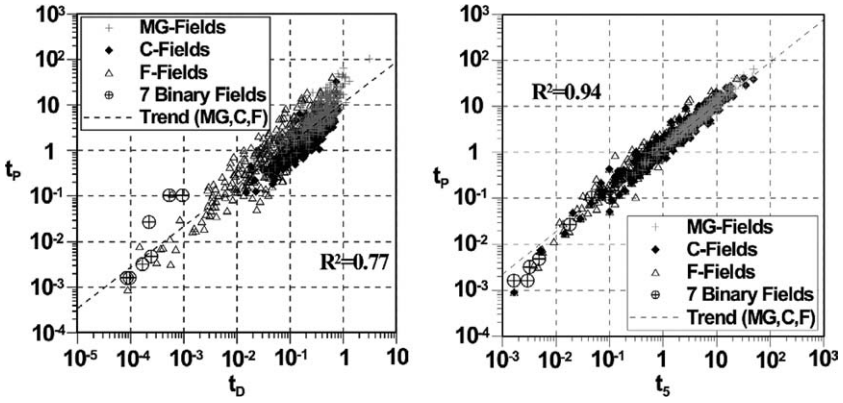

Figure 8 Comparison of the travel time along the fastest path, t_P, to both the drawdown response time, t_D (left), and the tracer travel time, t_5 (right). The linear correlation coefficients are based on all 1200 log-transformed value pairs.

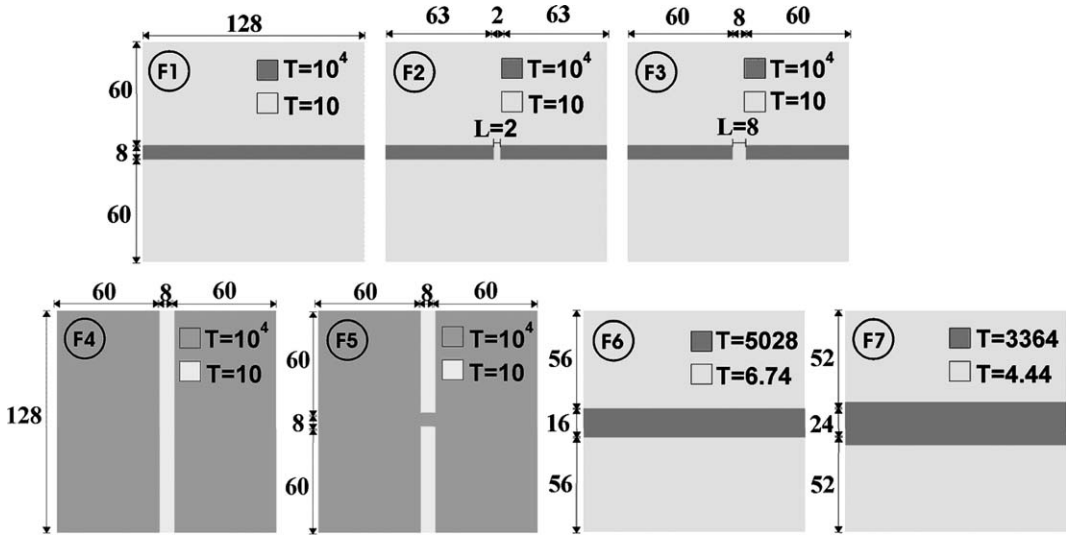

Figure 9 Seven binary fields, F1—F7, that help illustrate fundamental differences between apparent diffusivity, and flow and transport connectivity. The values of flow and transport connectivity indicators and related parameters for the seven fields are presented in Table 3.

The path of least resistance, and thus t_P, is identical for fields F3 and F4 (straight line through the center). Since the flow through F4 is uniform, $t_5 = t_P$ for F4. For F3 t_5 is about half the value of t_P. This may seem contradictory as T_{eff} is almost five times higher for F4 than for F3 (one would therefore expect t_5 in F4 to be much smaller than for F3). F1 and F5 comprise a similar example. They also have identical paths of least resistance, but nevertheless t_5 is more than twice as large for F5 as for F1 despite the fact that F5 has a significantly higher T_{eff} than F1. In both cases, a qualitative, somewhat simplified explanation is that tracer travel velocity and thus early tracer arrival is controlled by the width of the channel that accommodates the early arriving tracer. A narrow channel decreases t_5, whereas a wide channel increases in t_5.

F6 and F7 are constructed so that they display the same T_{eff} as F1. The three fields have been assigned the same actual storativity (for the sake of the example set to unity). As the three fields display identical T_{eff} and S, one would expect the interpretation of a pumping test using Jacob's method to yield similar estimates of the diffusivity and little information on the internal geometry. Indeed, the flow connectivity indicator CF is the same for the three fields. However, as seen from Table 1, both CT and D_R are significantly larger for F1 than for F6 and F7. This illustrates that (1) even for media with identical T_{eff} and S, D_R can provide some insight with respect to differences in internal geometry, that (2) D_R and CT seem to respond in a qualitatively similar way to heterogeneity that control early arrival time, and that (3) transport connectivity seems to depend more on the narrowness of the high-T channel than does flow connectivity.

F1, F2, and F3 are different only with respect to the size of the gap which breaks up the high-T channel crossing them from left to right. Table 1 shows that CF is greatly reduced by such a gap — from 41.2 to 4.28 or 2.20 depending on the gap size (see also Knudby et al., 2006). In contrast, CT is only reduced by a factor smaller than 1.5. This suggests that the presence of a low-T zone along an otherwise continuous high-T channel affects flow connectivity more than trans-

Table 3 Parameter values for the seven fields depicted in Fig. 9

	F1	F2	F3	F4	F5	F6	F7
T_{eff}	634	65.4	33.0	156	2939	634	634
T_G	15.4	15.3	15.0	6494	6671	15.4	15.4
T_P	10,000	597.6	156.4	156.4	10,000	5028	3364
CF (T_{eff}/T_G)	41.2	4.28	2.20	2.40×10^{-2}	4.41×10^{-1}	41.2	41.2
t_{AVE}	2.55×10^{-2}	2.48×10^{-1}	4.93×10^{-1}	1.03×10^{-1}	5.53×10^{-3}	2.55×10^{-2}	2.55×10^{-2}
t_5	1.63×10^{-3}	1.81×10^{-2}	4.62×10^{-2}	1.03×10^{-1}	2.94×10^{-3}	3.23×10^{-3}	4.82×10^{-3}
t_D	8.40×10^{-5}	2.22×10^{-4}	9.41×10^{-4}	5.34×10^{-4}	9.54×10^{-5}	1.66×10^{-4}	2.44×10^{-4}
t_P	1.63×10^{-3}	2.72×10^{-2}	1.03×10^{-1}	1.03×10^{-1}	1.63×10^{-3}	3.23×10^{-3}	4.82×10^{-3}
CT (t_{AVE}/t_5)	15.8	13.8	10.6	1.00	1.88	7.87	5.27
D_R	679	259	62.9	0.256	1.40	349	236

port connectivity. The presence of the gap reduces D_R less than CF, but more than CT. Comparison of F2 and F7 also lends some support to the above observations on the effects of channel discontinuities and channel narrowness. Despite the discontinuity in the high-T channel in F2, it has a higher CT and D_R than F7. The channel discontinuity, however, causes CF to be significantly lower for F2 than for F7. F4 and F5 were constructed to analyze the effect of a bottleneck. The two fields are different only with respect to the gap in a low-T barrier perpendicular to the flow direction. As compared to F4, the gap in F5 causes CF to increase by a factor 18, whereas CT increases by a factor of less than 2. Again, D_R falls in between as it increases with a factor 5.6. The behavior of CF, CT, and D_R show the same tendency as for F1, F2, and F3, namely that CF is more dependent on the continuity of the connected features than CT, and that D_R, in this respect, lies somewhere in between.

The simplicity of the above analysis of the seven binary fields prevents firm conclusions. Nevertheless the results consistently suggest that continuity of high-T channels is more of a requirement for high flow connectivity than for high transport connectivity, and that channel narrowness affects transport connectivity more than flow connectivity. Also, it is worth noticing that the seven binary fields ''comply'' with the relationships analyzed for correlation coefficients for the Gaussian fields, see Figs. 6 and 8. This shows that although the binary and the MG-, C- and F-fields are structurally very different, they react similarly to differences in connectivity.

Discussion

The analysis of the correlation between arrival times showed that $\log(D_R)$ is strongly, and approximately linearly, correlated to $\log(CF \cdot CT)$. This explains the observation that D_R reacts to differences in connectivity in a way that is intermediate to CF and CT. Since CF accounts for the flow rate increase due to connected features, whereas CT accounts for early arrival as compared to the average arrival time, D_R can be seen as accounting in an integrated way for both flow and transport connectivity. In terms of tracer movement, D_R correlates well with the time of early tracer arrival because it accounts both for connectivity effects controlling the average plume movement (through CF) and for connectivity effects not linked to the effective medium properties that control the progression of the solute front (through CT).

The logarithm of the tracer travel time, t_5, was found to be linearly correlated to the logarithm of the travel time of the drawdown signal, t_D. The trend line was found to have a slope of 1. This is in accordance with results of Paris (2002), Herweijer (1996a,b). The similar travel time comparison of Herweijer (1996a) was based on three-dimensional convergent flow and conductivity distributions representing a simple facies model and Gaussian and nested Gaussian random fields realizations. Paris (2002) presents a similar analysis for three-dimensional convergent flow to a central well in a cylinder shaped fracture system. In other words, the systems analyzed by Herweijer (1996a), Paris (2002) and the type of fields analyzed in the present study are different both in terms of dimensionality, flow domain and the type of geological medium they represent. The fact that the strong correlation is observed in all cases therefore suggests that such strong correlation between early tracer arrival and early drawdown response can be assumed for most types of hydrogeologic systems. Herweijer (1996a) analyzed the correlation between the tracer travel time and t_D using different fractions of the total amount of tracer (5%, 15%, 50%, and 75% — we use 5%) when determining the breakthrough time. Both the correlation coefficient and the slope of the approximately linear log—log relationship was found to decrease with increasing tracer fraction. In advection dominated systems, increased dispersion can be expected to have limited effect on t_5. However, dependent on the degree of connectivity, it can be expected to cause increased tailing and thus an increase in t_{AVE} and CT (e.g. Zinn and Harvey, 2003; Zheng and Gorelick, 2003). Paris (2002) found that matrix diffusion has very little effect on the correlation between D_R and CT. Sánchez-Vila and Carrera (2004) found that dispersion and matrix diffusion can lead to breakthrough curves which can be difficult to distinguish. It is therefore reasonable to expect good correlation between CT and D_R also in the presence of dispersion. In other words, the strong correlation between the two types of response times cannot only be assumed for most types of hydrogeologic systems, but also in the presence of matrix diffusion and small scale dispersion and, within limits, also independently of the exact definition of what constitutes an early breakthrough. This again supports the conjecture that D_R could potentially be useful for predicting early tracer arrival in most hydrogeologic systems.

Although the correlation between hydraulic response and tracer arrival times was found to be strong it does not allow for actual inference of solute travel time. The drawdown response is affected by the actual storativity, whereas solute arrival is controlled by the effective porosity. The two types of arrival times can therefore not be expected to correspond. We conjecture that it might be possible to remedy this by first determining a relevant relationship between tracer arrival times and drawdown signal arrival times over shorter distances and, subsequently, using such a relationship combined with a pumping test over larger distances to estimate solute arrival times for larger distances.

The objective of the present study is to analyze the relevance of D_a, and therefore S_a, as indicators of connectivity. We have based the above analysis on D_R ($D_R = D_a/(T_G/S)$). Since both D_a and T_{eff}/S_a are inversely proportional to t_0, the information contents in D_a is identical to that in T_{eff}/S_a. However, this does not entail that S_a (when estimated using Jacob's method) correlates as well with CT or $CF \cdot CT$ as does D_a. This is so because T_{eff} (actually T_{eff}/T_G) contains information on connectivity independently of S_a and D_a. We found poor correlation between $S_a = T_{eff}/D_a$ and CT and also between $S_a = T_{eff}/D_a$ and $CF \cdot CT$. In other words, D_a is useful for describing the combined effects of flow and transport connectivity, whereas S_a (when estimated using Jacob's method) is less useful for this purpose as it already carries connectivity information through T_{eff}. We therefore suggest using D_a instead of S_a.

Conclusions

Several previous studies have found that the storativity estimated from interpretation of pumping tests using Jacob's method contain information on the degree of hydraulic interconnectedness between the pumping and the observation well rather than represent actual storativity. As a consequence, both the apparent storativity, S_a, and the related dimensionless apparent hydraulic diffusivity, D_R ($D_R = D_a/(T_G/S)$) could potentially be valuable as indicators of connectivity. However, only visual (and thus undefined) notions of connectivity have been so far been used to study the relationship between apparent diffusivity and connectivity. The objective of the present paper is to use defined and quantifiable measures of connectivity to test the relevance of using S_a and D_a as indicators of connectivity. In addition we investigate how S_a and D_a are related to two indicators of flow and transport connectivity (CF and CT) analyzed in (Knudby and Carrera, 2005).

For the eight series of 150 fields displaying varying degrees of connectivity used in the present study, D_R increases with increased connectivity. In accordance with the findings of previous studies we therefore conclude that the apparent hydraulic diffusivity contains significant information on connectivity and that it is relevant to use it as an indicator of connectivity.

An indicator of transport connectivity, CT (t_{AVE}/t_5), was shown to correlate better with D_R than with an indicator of flow connectivity CF (T_{eff}/T_G). At the same time, the correlation between D_R and CT was found to be weaker than the correlation between D_R and CF. This indicates that although D_R provides more information on transport connectivity than does the flow connectivity indicator CF, it is at the same time strongly related to the channeling of flow. In other words, D_R could be a valuable source of information on the tendency to early arrival. When tracer tests provide early arrival time information for short distances, the use of D_R estimated from pumping tests covering larger distances could be useful for estimating travel times over larger distances.

The logarithm of D_R was found to be strongly, and approximately linearly, correlated to the logarithm of the product of CF and CT. This explains the observation that D_R reacts to differences in connectivity in a way which is intermediate to CF and CT. In terms of tracer movement, D_R correlates well with the time of early tracer arrival because it accounts both for connectivity effects controlling the average plume movement (through CF) and for connectivity effects not linked to the effective medium properties that control the progression of the solute front (through CT).

An analysis of seven idealized binary fields suggested that flow connectivity hinges more on the continuity of the fast paths, whereas transport connectivity seems to be more dependent on the width of the connected features forming, possibly discontinuous, fast paths. The analysis of the seven fields supported the conjecture that D_R does indeed contain information on connectivity and indicated that D_R depends on fast path continuity and channel width in an intermediate manner as compared to CF and CT.

For hydrologic systems qualitatively quite different from the ones studied in the present paper, Herweijer (1996a,b), Paris (2002) found very good correlation between the times of the hydraulic response and of early tracer arrival. In accordance with these results, we consistently found strong correlation between the two types of arrival times. Together the results suggest that such strong correlation between early tracer arrival and drawdown response can be assumed for most types of hydrogeologic systems.

In order to analyze in more detail the path followed by the two types of signals, the path of least resistance was determined and compared to the paths followed by the fastest packages of tracer and the fastest part of the ''line of depression''. The travel time corresponding to the path of least resistance, t_P, was found to correlate well with both the arrival time of 5% of the tracer, t_5, and the arrival time of the ''line of depression'', t_D. Strong correlation and approximate correspondence between the values of t_P and t_5 suggests that t_P could be useful for estimating early arrival time.

Acknowledgements

Funding for the above work was provided by The Danish Research Agency and The Spanish Nuclear Waste Management Agency (ENRESA).

References

Alabert, F.G., Aquitaine, E., Modot, V. 1992. Stochastic models of reservoir heterogeneity: Impact on connectivity and average permeabilities. Soc. Pet. Eng. Tech. Paper 24893, pp. 355–370.

Ambegaokar, V., Halperin, B.I., Langer, L.S., 1971. Hopping conductivity in disordered systems. Physical Review B 4 (8), 2612–2620.

Anderson, M.P., Woessner, W.W., 1992. Applied Groundwater Modeling. Academic Press, San Diego.

Beckie, R., Harvey, C.F., 2002. What does a slug test measure: An investigation of instrument response and the effects of heterogeneity. Water Resources Research 38 (12), 1290. doi:10.1029/2001WR001072.

Bohling, G.C., Zhan, X., Butler Jr., J.J., Zheng, L., 2002. Steady shape analysis of tomographic pumping tests for characterization of aquifer heterogeneities. Water Resources Research 38 (12), 1324. doi:10.1029/2001WR001176.

Brauchler, R., Liedl, R., Dietrich, P., 2003. A travel time based hydraulic tomographic approach. Water Resources Research 39 (12), 1370. doi:10.1029/2003WR002262.

Bruderer-Weng, C., Cowie, P., Bernabe, Y., Main, I., 2004. Relating flow channeling to tracer dispersion in heterogeneous networks. Advances in Water Resources 27, 843–855.

Butler Jr., J.J., McElwee, C.D., Bohling, G.C., 1999. Pumping tests in networks of multilevel sampling wells: Motivation and methodology. Water Resources Research 35 (11), 3553–3560.

Carslaw, H.S., Jaeger, J.C., 1959. Conduction of Heat in Solids, second ed. Oxford University Press, New York.

Cherkassky, B.V., Goldberg, A.V., Radzik, T., 1996. Shortest paths algorithms: Theory and experimental evaluation. Mathematical Programming 73, 129–174.

Cooper, H.H., Jacob, C.E., 1946. A generalized graphical method for evaluating formation constants and summarizing well field history. American Geophysical Union Transactions 27, 526–534.

Deutsch, C.V., Journel, A., 1992. GSLIB. Geostatistical Software Library. Oxford University Press, New York.

Dijkstra, E.W., 1959. A note on two problems in connection with graphs. Numeriche Mathematik 1, 269–271.

Fernandez-Garcia, D., Sánchez-Vila, X., Illangasekare, T.H., 2002. Convergent-flow tracer tests in heterogeneous media: combined experimental–numerical analysis for determination of equivalent transport parameters. Journal of Contaminant Hydrology 57, 129–145.

Fetter, C.W., 2000. Applied Hydrogeology. Prentice Hall, Englewood Cliffs, NJ.

Fogg, G.E., 1986. Groundwater flow and sand body interconnectedness in a thick, multiple-aquifer system. Water Resources Research 22 (5), 679–694.

Fogg, G.E., Senger, R.K., 1985. Automatic generation of flow nets with conventional ground-water modeling algorithms. Groundwater 23 (3), 336–344.

Fogg, G.E., Carle, S.F., Green, C., 2000. Connected-network paradigm for the alluvial aquifer system. In: Zhang, D., Winter, C.L. (Eds.), Theory, Modeling, and Field Investigation in Hydrogeology: A Special Volume in Honor of Shlomo P. Neuman's 60th Birthday, Boulder, Colorado, Geological Society of America Special Paper 348, pp. 25–42.

Freeze, R.A., Cherry, J.A., 1979. Groundwater. Prentice-Hall, Englewood Cliffs, NJ.

Frind, E.O., Matanga, G.B., 1985. The dual formulation of flow for contaminant transport modeling: 1. Review of theory and accuracy aspects. Water Resources Research 21 (2), 159–169.

Gómez-Hernández, J.J., Wen, X.-H., 1998. To be or not to be multi-Gaussian. A reflection on stochastic hydrogeology. Advances in Water Resources 21 (1), 47–61.

Gómez-Hernández, J.J., Sovero, H., Sahuquillo, A., 1995. Some issues on the analysis of pumping tests in heterogeneous aquifers. Hidrogeologie 3, 13–18.

Gómez-Hernández, J.J., Sahuquillo, A., Capilla, J.E., 1997. Stochastic simulation of transmissivity fields conditional to both transmissivity and piezometric data – 1. Theory. Journal of Hydrology 203, 162–174.

Grayson, R.B., Blöschl, G., Western, A.W., McMahon, T.A., 2002. Advances in the use of observed spatial patterns of catchment hydrological response. Advances in Water Resources 25, 1314–1334.

Guimerá, J., Carrera, J., 2000. A comparison of hydraulic and transport parameters measured in low-permeability fractured media. Journal of Contaminant Hydrology 41, 261–281.

Guswa, A.J., Freyberg, D.L., 2002. On using the equivalent conductivity to characterize solute spreading in environments with low-permeability lenses. Water Resources Research 30 (8). doi:10.1029/2001WRR000528.

Harbaugh, A.W., Banta, E.R., Hill, M.C.,McDonald, M.G., 2000. MODFLOW-2000, The US Geological Survey Modular Ground-Water Model – User Guide to Modularization Concepts and The Ground-Water Flow Process. Open-File Report 00-92, United States Geological Survey, Boulder, Colorado, 121 p.

Herrera, I., Yates, R., 1977. Integrodifferential equations for systems of leaky aquifers and applications. 3. Numerical Method of unlimited applicability. Water Resources Research 13 (4), 725–732.

Herweijer, J.C., 1996a, Constraining uncertainty of groundwater flow and transport models using pumping tests. In: Calibration and Reliability in Groundwater Modelling, Proceedings ModelCARE 96, Golden, Colorado, 24–26 September 1996, pp. 473–482.

Herweijer, J.C., 1996b. Sedimentary Heterogeneity and Flow Towards a Well. Assessment of Flow Through Heterogeneous Formations. PhD dissertation, Free University of Amsterdam.

Herweijer, J.C., Young, S.C., 1991. Use of detailed sedimentological information for the assessment of aquifer tests and tracer tests in a shallow fluvial aquifer. In: Proceedings of the Fifth Annual Canadian American Conference on Hydrogeology, Calgary, 18–20 September 1990. NWWA, Dublin, OH, pp. 101–115.

Hunt, A.G., 2001. Applications of percolation theory to porous media with distributed local conductances. Advances in Water Resources 24, 279–307.

Illman, W.A., Tartakovsky, D.M., 2005. Asymptotic analysis of three-dimensional pressure interference tests: A line-injection line-monitoring solution. Advances in Water Resources 28 (11), 1217–1229.

Journel, A.G., Deutsch, C.V., 1993. Entropy and spatial disorder. Mathematical Geology 25 (3), 329–355.

Knudby, C., Carrera, J., 2005. On the relationship between indicators of geostatistical, flow and transport connectivity. Advances in Water Resources 28 (4), 405–421.

Knudby, C., Carrera, J., Bumgardner, J., Fogg, G., 2006. Binary upscaling – the role of connectivity and a new formula. Advances in Water Resources 29 (4), 590–604.

Lee, S.-Y., 2004. Heterogeneity and Transport: Geostatistical Modeling, Non-Fickian Transport, and Efficiency of Remediation Methods. PhD Dissertation, University of California, Davis.

Martinez-Landa, L., Carrera, J., 2005. An analysis of hydraulic conductivity scale effects in granite (Full-scale Engineered Barrier Experiment (FEBEX), Grimsel, Switzerland). Water Resources Research 41, W03006. doi:10.1029/2004WR003458.

Matheron, G., 1967. Eléments pour une Théorie des Milieux Poruex. Masson, Paris.

Meier, P.M., Carrera, J., Sánchez-Vila, X., 1998. An evaluation of Jacob's method for the interpretation of pumping tests in heterogeneous formations. Water Resources Research 34 (5), 1011–1025.

Meier, P.M., Carrera, J., Sánchez-Vila, X., 1999. A numerical study of the relationship between transmissivity and specific capacity in heterogeneous aquifers. Groundwater 37 (4), 611–617.

Meier, P.M., Medina, A., Sánchez-Vila, X., 2001. Geostatistical inversion of cross-hole pumping tests for identifying preferential flow channels within a shear zone. Groundwater 39 (1), 10–17.

Neuweiler, I., Cirpka, O.A., 2005. Homogenization of Richards equation in permeability fields with different connectivities. Water Resources Research 41 (2). doi:10.1029/2004WR003329.

Paris, B., 2002. Aspo Hard Rock Laboratory, International Progress Report IPR-02-16, Itasca Consultants, S.A. for Swedish Nuclear Fuel and Waste Management Co.

Ptak, T., Piepenbrink, M., Martac, E., 2004. Tracer tests for the investigation of heterogeneous porous media and stochastic modelling of flow and transport — a review of some recent developments. Journal of Hydrology 294, 122—163.

Rutqvist, J., Noorishad, J., Tsang, C.-F., Stephansson, O., 1998. Determination of fracture storativity in hard rocks using high-pressure injection testing. Water Resources Research 34 (10), 2551—2560.

Sánchez-Vila, X., Carrera, J., 2004. On the striking similarity between the moments of breakthrough curves for a heterogeneous medium and a homogeneous medium with a matrix diffusion term. Journal of Hydrology 294, 164—175.

Sánchez-Vila, X., Carrera, J., Girardi, J.P., 1996. Scale effects in transmissivity. Journal of Hydrology 183, 1—22.

Sánchez-Vila, X., Meier, P.M., Carrera, J., 1999a. Pumping tests in heterogeneous aquifers: An analytical study of what can be obtained from their interpretation using Jacob's method. Water Resources Research 35 (4), 943—952.

Sánchez-Vila, X., Axness, C.L., Carrera, J., 1999b. Upscaling transmissivity under radially convergent flow in heterogeneous media. Water Resources Research 35 (3), 613—621.

Schad, H., Teutsch, G., 1994. Effects of the investigation scale on pumping test results in heterogeneous porous aquifers. Journal of Hydrology 159, 61—77.

Scheibe, T.D., Yabusaki, S., 1998. Scaling of flow and transport behavior in heterogeneous groundwater systems. Advances in Water Resources 22 (3), 223—238.

Silliman, S.E., 1996. The importance of the third dimension on transport through saturated porous media: case study based on transport of particles. Journal of Hydrology 179, 181—195.

Vandenbohede, A., Lebbe, L., 2003. Combined interpretation of pumping and tracer tests: theoretical considerations and illustration with a field test. Journal of Hydrology 277 (1—2), 134—149.

Vasco, D.W., Keers, H., Karasaki, K., 2000. Estimation of reservoir properties using transient pressure data: An asymptotic approach. Water Resources Research 36 (12), 3447—3465.

Vesselinov, V.V., Neuman, S.P., Illman, W.A., 2001. Three-dimensional numerical inversion of pneumatic cross-hole tests in unsaturated fractured tuff: 2. Equivalent parameters, high-resolution stochastic imaging, and scale effects. Water Resources Research 37 (12), 3019—3041.

Walton, W.C., 1987. Groundwater Pumping Tests: Design and Analysis. Lewis Publishers, Inc..

Warren, J.E., Price, H.H., 1961. Flow in heterogeneous porous media. Society of Petroleum Engineers Journal 1, 153—169.

Wen, X.-H., Gómez-Hernandez, J.J., 1996. Upscaling hydraulic conductivities in heterogeneous media: An overview. Journal of Hydrology 183, ix—xxxii.

Wen, X.H., Gómez-Hernández, J., 1998. Numerical modeling of macrodispersion in heterogeneous media — a comparison of multi-Gaussian and non-multi-Gaussian models. Journal of Contaminant Hydrology 30 (1—2), 129—156.

Western, A.W., Blöschl, G., Grayson, R.B., 2001. Toward capturing hydrologically significant connectivity in spatial patterns. Water Resources Research 37 (1), 83—97.

Yeh, T.-C.J., Liu, S., 2000. Hydraulic tomography: Development of a new aquifer test method. Water Resources Research 36 (8), 2095—2105.

Zheng, C., Gorelick, S.M., 2003. Analysis of solute transport in flow fields influenced by preferential flowpaths at the decimeter scale. Ground Water 41 (2), 142—155.

Zinn, B., Harvey, C.F., 2003. When good statistical models of aquifer heterogeneity go bad: A comparison of flow, dispersion, and mass transfer in connected and multivariate Gaussian hydraulic conductivity fields. Water Resources Research 39 (3), 1051. doi:10.1029/2001WR001146.